Published in final edited form as:
J Cell Sci. 2008 October 1; 121(0 19): 3133–3139. doi:10.1242/jcs.034496.

Cytosolic Ca^{2+} prevents the subplasmalemmal clustering of STIM1: an intrinsic mechanism to avoid Ca^{2+} overload

Roland Malli[1], **Shamim Naghdi**[1], **Christoph Romanin**[2], and **Wolfgang F. Graier**[1,*]

[1]Institute of Molecular Biology and Biochemistry, Center of Molecular Medicine, Medical University of Graz, Graz, Austria

[2]Institute of Biophysics, University of Linz, Linz, Austria

Summary

The stromal interacting molecule (STIM1) is pivotal for store-operated Ca^{2+} entry (SOC). STIM1 proteins sense the Ca^{2+} concentration within the lumen of the endoplasmic reticulum (ER) via an EF-hand domain. Dissociation of Ca^{2+} from this domain allows fast oligomerization of STIM1 and the formation of spatially discrete clusters close to the plasma membrane. By lifetime-imaging of STIM1 interaction, the rearrangement of STIM1, ER Ca^{2+} concentration ($[Ca^{2+}]_{ER}$) and cytosolic Ca^{2+} signals ($[Ca^{2+}]_{cyto}$) we show that $[Ca^{2+}]_{cyto}$ affects the subcellular distribution of STIM1 oligomers and prevents subplasmalemmal STIM clustering, even if the ER is depleted. These data indicate that $[Ca^{2+}]_{cyto}$, independently of the ER Ca^{2+} filling state, crucially tunes the formation and disassembly of subplasmalemmal STIM1 clusters, and, thus, protects cells against Ca^{2+} overload resulting from excessive SOC activity.

Keywords

ER Ca^{2+} dynamics; FRET; STIM1 oligomerization; Store-operated Ca^{2+} entry

Introduction

Store-operated Ca^{2+} entry (SOC) (Putney, 1986; Putney, 1990) is activated upon ER Ca^{2+} depletion in almost every cell type and is crucial for the regulation of manifold Ca^{2+}-sensitive cellular processes (Parekh and Putney, 2005). Recently, STIM1 was identified as key mediator for SOC channel activation (Liou et al., 2005; Mercer et al., 2006; Roos et al., 2005). STIM1, which is homogeneously embedded in the ER membrane where under resting conditions (Dziadek and Johnstone, 2007), functions as a sensor of $[Ca^{2+}]_{ER}$ via a luminal EF-hand Ca^{2+} binding domain (Liou et al., 2005; Roos et al., 2005). Upon ER depletion, Ca^{2+} dissociates from STIM1 yielding its homo-oligomerization, which is prerequisite for the assembly of subplasmalemmal STIM1 clusters that trigger activation of Ca^{2+} permeable SOC channels (Liou et al., 2005; Roos et al., 2005). Notably, even during the formation of subplasmalemmal STIM1 clusters, STIM1 remains in the ER environment (Hewavitharana et al., 2007) and translocates to ER-plasma membrane junctions along

*Author for correspondence (wolfgang.graier@meduni-graz.at).

Europe PMC Funders Author Manuscripts

microtubular structures (Smyth et al., 2007) under the assistance of the microtubule-plus-end-tracking protein, EB1 (Grigoriev et al., 2008).

The primary role of SOC is supposed to be the maintenance of cytosolic Ca^{2+} signals and the replenishment of intracellular Ca^{2+} stores (Parekh, 2003). However, in endothelial cells, alternative agonist-triggered Ca^{2+} entries (Jousset et al., 2008; Nilius et al., 2003) and Ca^{2+} entry pathways exist [e.g. Na^+/Ca^{2+} exchanger (Graier et al., 1995)]. Notably, simultaneous stimulation of multiple Ca^{2+} entry mechanisms might entail the risk of cellular Ca^{2+} overload that, at worst, can result in cell death (Berridge et al., 2000). Accordingly, it remains unclear whether STIM1 activity is subject to control by other processes, besides ER Ca^{2+} depletion, that impede activation of SOC when other Ca^{2+} entry mechanisms are active and prevent cellular Ca^{2+} overload, or whether STIM1 is active under normal physiological conditions. In this work, we intended to investigate the hypothesis that high $[Ca^{2+}]_{cyto}$ represents an important physiological regulator of STIM1 function by anticipating its full activation when ER Ca^{2+} is depleted.

Results and Discussion

ER Ca^{2+} depletion correlates with STIM1 oligomerization, whereas subplasmalemmal STIM1 clustering is delayed and follows the decay of cytosolic Ca^{2+} levels

As in most non-excitable cells, maximal ER Ca^{2+} depletion in endothelial cells is effectively accomplished by the generation of Ins(1,4,5)P_3 upon histamine-mediated stimulation in Ca^{2+}-free solution (Fig. 1A,E). Under such conditions, STIM1 oligomerization, measured as dynamic changes in FRET between CFP- and YFP-STIM1, perfectly correlated with ER Ca^{2+} depletion (Fig. 1H, left panel) and persisted as long as $[Ca^{2+}]_{ER}$ was low. However, it decreased rapidly upon re-addition of Ca^{2+} (Fig. 1B,E).

In addition to STIM1 oligomerization, the formation of subplasmalemmal STIM1 clusters was quantified by the redistribution of STIM1-YFP from deeper ER towards the subplasmalemmal area at distinct regions (supplementary material Fig. S1). Upon ER Ca^{2+} depletion, subplasmalemmal clustering (Fig. 1C,E) was significantly delayed compared with STIM1 oligomerization (Fig. 1B), indicating that oligomerization (phase I, Fig. 1F) occurs upstream of subplasmalemmal clustering (phase II, Fig. 1F). Notably, STIM1 clustering was accomplished by the translocation of STIM1 oligomers from the deep ER towards superficial ER domains without affecting the degree of oligomerization (supplementary material Fig. S1), indicating that STIM1 clusters consist of oligomers. Moreover, the formation of subplasmalemmal STIM1 clusters did not correlate with the kinetics of ER depletion but with the decay of cytosolic-free Ca^{2+} levels (Fig. 1H, right panel). These findings are in line with recent reports that delayed formation of STIM1 puncta after STIM1 oligomerization occurs in HeLa cells upon ER Ca^{2+} depletion with ionomycin (Liou et al., 2007). Moreover, these data also point to a modulatory role of cytosolic Ca^{2+} for STIM1 clustering.

Ca^{2+} readdition after washout of histamine rapidly elevated $[Ca^{2+}]_{cyto}$ (Fig. 1D,E) and accomplished ER Ca^{2+} cyto replenishment within 2 minutes (Fig. 1A), indicating SOC activity was present (Jousset et al., 2008). Notably, there was no kinetic difference between

the disassembly of subplasmalemmal STIM1 clusters (Fig. 1C) and the reduction in STIM1 oligomerization (Fig. 1B). These findings were further supported by calculating the effective correlation concentrations (ECC_{50}) of STIM1 oligomerization upon ER Ca^{2+} depletion ($ECC_{50/oligomerization}$) and ER Ca^{2+} refilling ($ECC_{50/disassembly}$). $ECC_{50/oligomerization}$ was found to be 192.7 (180.9-205.3) μM (n=9 for STIM1 oligomerization; n=10 for $[Ca^{2+}]_{ER}$) and was significantly higher (P>0.05) than the calculated $ECC_{50/disassembly}$ of 143.5 (129.8-158.6) μM (n=9 for STIM1 oligomerization; n=10 for $[Ca^{2+}]_{ER}$) (supplementary material Fig. S2). The observed kinetic differences between STIM1 oligomerization and STIM1 clustering in their initiation but not their termination (Fig. 1B,C) point to different processes in the regulation of subplasmalemmal STIM1 dynamics. This hypothesis seems feasible if one considers that the disassembly/degradation of STIM1 oligomers/clusters might be influenced by interaction with additional partners, such as Orai1 (Zhang et al., 2006), TRP(s) (Yuan et al., 2007), calmodulin (Bauer et al., 2008) and/or so far unknown scaffolds. In line with this assumption, our findings that STIM1 disassembly/degradation did not entirely resume baseline levels upon Ca^{2+} readdition/complete ER refilling (Fig. 1A-D) may indicate the lack of adequate availability of such interacting partners. These partners are imperative for proper disassembly/degradation of STIM1 oligomers/clusters in STIM1-overexpressing cells.

Upon cell stimulation under physiological conditions the recruitment of STIM1 is limited

We have previously reported that, in the presence of extracellular Ca^{2+}, stimulation with an Ins(1,4,5)P_3-generating agonist yields only moderate ER Ca^{2+} depletion (Fig. 2A,E) because of efficient back-cycling of Ca^{2+} to the ER (Malli et al., 2003b; Malli et al., 2005). Accordingly, the oligomerization of STIM1 and its subsequent subplasmalemmal clustering are assumed to be limited under these physiological conditions. In line with this expectation, in the present study, histamine failed to enhance STIM1 oligomerization in the presence of extracellular Ca^{2+}, whereas removal of extracellular Ca^{2+} induced this process (Fig. 2B,E). Moreover, basal STIM1 oligomerization rates declined upon stimulation with histamine in the presence of extracellular Ca^{2+} in three out of 11 experiments. Consistently, cytosolic Ca^{2+} elevation in response to histamine in Ca^{2+}-containing buffer (Fig. 2D,E) was associated with pronounced degradation of pre-existing subplasmalemmal STIM1 clusters (supplementary material Fig. S3, Movie 1).

Intriguingly, repetitive subplasmalemmal clustering of STIM1 occurred at identical distinct areas (Fig. 2F). As the spatially allocated repetitive formation of STIM1 clusters was observed even 15 minutes after their disaggregation, it is tempting to speculate that the STIM1 oligomers are directed and/or attracted by elements of the cytoskeleton [e.g. EB1 (Grigoriev et al., 2008)], plasma membrane-associated anchor proteins [e.g. INAD (Chevesich et al., 1997)] and/or plasma membrane ion channels [e.g. Orai1 (Muik et al., 2008; Peinelt et al., 2006)].

As the global ER Ca^{2+} content is slightly but significantly reduced upon cell stimulation with histamine in Ca^{2+}-containing buffer (Fig. 2A), these findings challenge the hypothesis that ER Ca^{2+} depletion is the exclusive instigator for STIM1 recruitment to plasma membrane Ca^{2+} channels. Nevertheless, the observed decomposition of subplasmalemmal

STIM1 clusters might be due to a redistribution of Ca^{2+} from deep ER towards discrete superficial ER domains. As superficial ER domains are predominantly depleted upon histamine stimulation (Frieden et al., 2002; Malli et al., 2003a), such luminal Ca^{2+} redistribution within the ER seems unlikely. Hence, during the course of these studies, the generation of very high Ca^{2+} gradients within superficial ER domains and the plasma membrane upon cell stimulation were reported (Frieden et al., 2002; Malli et al., 2003a); thus, pointing to superficial Ca^{2+} gradients as a mediator for the disassembly of subplasmalemmal STIM1 clusters.

Cytosolic Ca^{2+} represents a main determinant for the stability of subplasmalemmal STIM1 clusters and maintenance of SOC activity

In order to explore whether or not cytosolic Ca^{2+} contributes to STIM1 dynamics by promoting disassembly of subplasmalemmal STIM1 clusters, STIM1 clustering was measured under conditions in which the agonist-induced Ca^{2+} elevation was buffered by BAPTA. In BAPTA-am-loaded cells (Fig. 3B, left images), neither basal $[Ca^{2+}]_{cyto}$ (Fig. 3C) nor the number and size of pre-existing subplasmalemmal STIM1 clusters (Fig. 3D) differed from cells without BAPTA-am loading (i.e. control cells) (Fig. 3A, left images). Notwithstanding, the cytosolic Ca^{2+} rise in response to histamine was largely prevented in BAPTA-loaded cells (Fig. 3C). This lack of cytosolic Ca^{2+} elevation in response to histamine was accompanied by the incompetence of this agonist to disassemble subplasmalemmal STIM1 clusters and even increased their formation (Fig. 3A,B, middle panels; Fig. 3D). The latter phenomenon is most probably due to the pronounced ER Ca^{2+} depletion in BAPTA-loaded cells as a consequence of increased cytosolic Ca^{2+} buffer capacity that impairs Ca^{2+} recycling into the ER.

In line with this assumption, increasing cytosolic Ca^{2+} buffer capacity with BAPTA enhances the extent and duration of SOC currents or I_{CRAC} (Gilabert and Parekh, 2000; Hoth et al., 1997; Parekh and Putney, 2005). These findings lead to the dogma that the SOC/I_{CRAC}-channel(s) is/are sensitive to local Ca^{2+} gradients at the inner mouth of these channels. However, considering that subplasmalemmal STIM1 clustering is prerequisite for SOC activity (Mercer et al., 2006; Muik et al., 2008), it is tempting to speculate that the Ca^{2+}-induced degradation of subplasmalemmal STIM1 clusters described herein is, at least partially, responsible for the Ca^{2+} sensitivity of SOC.

Subplasmalemmal clustering of oligomerized STIM1 is under the control of $[Ca^{2+}]_{cyto}$

So far, our experiments reveal cytosolic Ca^{2+} as determinant for the disassembly of subplasmalemmal STIM clusters, while the effect of $[Ca^{2+}]_{cyto}$ on the formation of STIM1 assemblies near the plasma membrane remains unexplored. Accordingly, the formation of subplasmalemmal STIM1 clusters was investigated in the presence of the SERCA inhibitor BHQ. This allowed us to study the kinetics of STIM1 clustering at various cytosolic Ca^{2+} concentrations (Fig. 4A), while the ER Ca^{2+} content was clamped to an almost completely emptied state (Fig. 4B). Consequently, under these conditions, STIM1 oligomerization was maximal, as indicated by the lack of a further effect upon removal of extracellular Ca^{2+} (Fig. 4C).

However, despite maximal STIM1 oligomerization and clustering, these proteins assemblies preferentially remained in the deep ER and did not accumulate close to the plasma membrane (Fig. 4D,E; Movie 2). Moreover, lowering $[Ca^{2+}]_{cyto}$ by removal of extracellular Ca^{2+} yielded strong accumulation of subplasmalemmal STIM1 clusters that followed their disassembly but not deoligomerization at deep ER domains (Fig. 4D-F, left panel). These data indicate that: (1) cytosolic Ca^{2+} does not affect STIM1 oligomerization upon ER Ca^{2+} depletion; (2) the subsequent formation of subplasmalemmal STIM1 clusters is prevented by elevated cytosolic Ca^{2+} levels independently from ER Ca^{2+} content; and (3) subplasmalemmal STIM1 clustering upon reduction of cytosolic Ca^{2+} requires previous disassembly of STIM1 clusters in the deep ER.

Moreover, subsequent readdition of extracellular Ca^{2+} that again raised $[Ca^{2+}]_{cyto}$ but not the ER Ca^{2+} content induced disassembly of subplasmalemmal STIM1 clusters and their reformation at the deeper ER without any effect on STIM1 oligomerization (data not shown). These findings suggest that an elevation of cytosolic Ca^{2+} destabilizes subplasmalemmal STIM1 clusters but not STIM1 oligomers. Accordingly, STIM1 exists in four different states: (1) as homogeneously distributed monomers at the entire ER under non-stimulated conditions; (2) as oligomers that are about to form clusters upon ER depletion; (3) as STIM1 clusters at the deep ER while $[Ca^{2+}]_{cyto}$ is elevated; and (4) as subplasmalemmal STIM1 clusters that couple to plasma membrane Ca^{2+} channels when $[Ca^{2+}]_{cyto}$ is low. In addition to these distinctively measurable states of STIM1, our data, that subplasmalemmal STIM1 clusters disassemble and reassemble in the deep ER while no change in STIM1 oligomerization occurs, allow us to assume that STIM1 oligomers exist as mobile intermediates between local clusters.

In view of our findings that the assembly of subplasmalemmal STIM1 clusters, most likely coupled to plasma membrane SOC channels (Muik et al., 2008), is tightly controlled by $[Ca^{2+}]_{cyto}$ indicates that SOC activation is thoroughly organized. Obviously, STIM1 oligomerization is triggered by ER Ca^{2+} depletion but this does not necessarily lead to subplasmalemmal STIM1 clustering and activation as this process is under the control of $[Ca^{2+}]_{cyto}$. Such a mechanism may be of particular physiological importance as it can serve as a ‘security measure’ to prevent cellular Ca^{2+} overload by tuning SOC upon significant ER Ca^{2+} depletion, especially if the ER Ca^{2+} replenishment is diminished (as can occur in response to cellular ATP deprivation).

So far, we have not been able to clarify the exact mechanisms by which cytosolic Ca^{2+} disassembles subplasmalemmal STIM1 clusters and how their formation is prevented. However, time scan imaging allowed analysis of the velocity of comet-like movements of STIM1 protein assemblies probably along microtubules, which were recently supposed to be crucial for ER remodeling and STIM1 redistribution upon ER Ca^{2+} depletion (Grigoriev et al., 2008; Smyth et al., 2007). Elevation of $[Ca^{2+}]_{cyto}$ by either histamine or a combination of histamine and BHQ in the presence of extracellular Ca^{2+} significantly reduced the velocity of comet-like STIM1 movements, which could be restored by adding of EGTA (Fig. 4F). Remarkably, the motility of mitochondria, which continuously move along microtubule in resting conditions, are similarly controlled by $[Ca^{2+}]$cyto (Yi et al., 2004),

whereas it remains to be elucidated whether or not both phenomena relate to the same Ca^{2+}-dependent microtubular process.

In conclusion, we describe a new aspect of the regulation of STIM1 dynamics that sheds light on the organization of STIM1 activation under physiological conditions. Specifically, our findings suggest that ER Ca^{2+} depletion triggers STIM1 oligomerization whereas $[Ca^{2+}]_{cyto}$ inhibits subplasmalemmal STIM1 clustering. Thus, the efficiency of Ca^{2+} entry is under the control of cytosolic free Ca^{2+}. Such sophisticated regulation of STIM1 may be crucial to avoid Ca^{2+} overload of cells and ensures that STIM1 is activated only under conditions that cause the failure of a cell to accomplish ER Ca^{2+} refilling from its own cytosolic Ca^{2+} source.

Materials and Methods

Cell culture, constructs and transfection

The human umbilical vein endothelial cell line EA.hy926 (at passage 45 and over) was used for this study. For more details, see supplementary material. Cells were cultured in Dulbecco's minimum essential medium (Invitrogen, Groningen, Netherlands) containing 10% fetal calf serum (PAA, Linz, Austria) and 1% HAT (5 mM hypoxanthin, 20 μM aminopterin, 0.8 mM thymidine; Invitrogen). cDNA for YFP-STIM1, CFP-STIM1 and $D1_{ER}$ were inserted in pcDNA 3 (Invitrogen). Cells (approximately 80% confluency) were transiently transfected with 1.5-2 μg of purified plasmid DNA for either YFP-STIM1 alone or in combination with CFP-STIM1 for FRET measurements or with $D1_{ER}$ for simultaneous $[Ca^{2+}]_{ER}$ recordings using TransFast (Promega, Vienna, Austria) as previously described (Trenker et al., 2007). Between 24 and 36 hours after transfection cells were used for experiments.

Buffers and chemicals

The Ca^{2+}-containing experimental buffer (EB) was composed of (in mM) 145 NaCl, 5 KCl, 2 $CaCl_2$, 1 $MgCl_2$, 10 D-glucose and 10 HEPES; pH was adjusted to 7.4 with NaOH. For experiments in Ca^{2+}-free solution, Ca^{2+}-free EB containing 1 mM EGTA was used.

Dynamic measurements of STIM1 oligomerization

STIM1 oligomerization was analyzed in cells co-expressing CFP-STIM1 and YFPSTIM1 [N-terminal FP fusions (Liou et al., 2007; Muik et al., 2008)] by following FRET dynamics between the two fluorophores (Liou et al., 2007; Muik et al., 2008), according to previous FRET measurements (Malli et al., 2005; Osibow et al., 2006). CFP-STIM1 was excited at 440±21 nm (440AF21, Omega Optical, Brattleboro, VT) and emission was collected simultaneously at 535 (FRET channel, Omega Optical) and 480 nm (CFP channel, Omega Optical) using an optical beam splitter (535 and 480 nm, Dual-View MicroImager, Optical Insights, Visitron Systems) as described previously (Frieden et al., 2002). To correct the decay in the F_{535}:F_{480} ratio during the experiments, which was probably due to unequal photobleaching or photochromism of the different fluorophores, the STIM1 oligomerization were expressed as the ratio of $(F_{535}/F_{480})/R_0$.

Detection of STIM1 clustering

Using a customized array confocal laser scanning fluorescence microscope (Paltauf-Doburzynska et al., 2004; Trenker et al., 2007), YFP-STIM1 was illuminated at 488 nm with a 150 mW Ar laser (Laser Physics, West Jordan, UT) and emission data were collected at 535 nm to resolve the spatial and temporal redistribution of YFPSTIM1. The rate of subplasmalemmal STIM1 clustering was expressed as ratio of YFP-STIM1 fluorescence (F_{535}) in plasma-membrane-close (1 μm) regions (F close to PM) and that in regions defining deep, plasma-membrane-far (>2 μM) ER domains ($F_{\text{deep ER}}$). All images were obtained at room temperature with a 63× (Plan-Apochromat, NA 1.4, Zeiss, Vienna, Austria) or 100× (α Plan-Fluar, NA 1.45, Zeiss) objective and image analyses were performed using Metamorph 5.0 (Molecular Devices, Visitron Systems, Puchheim, Germany).

Cytosolic Ca^{2+} measurements obtained simultaneously with STIM1 clustering

Changes in $[Ca^{2+}]_{\text{cyto}}$ were monitored using fura-2-am as previously described (Graier et al., 1992; Graier et al., 1998). For simultaneous measurements of STIM1 clustering and $[Ca^{2+}]_{\text{cyto}}$, YFP-STIM1 expressing cells were loaded with fura-2-am as previously described (Malli et al., 2007; Malli et al., 2003a). fura-2 and YFP-STIM1 were illuminated alternatively at 340 and 380 nm (fura-2), and 480 nm (YFP), and emission was monitored at 510 and 535 nm, respectively. Experiments were performed on an automated epi-fluorescence microscope system (Axiovert 200 M, Zeiss) that was equipped with 2 Ludl filter-wheel devices (Ludl Electronic Products, Hawthrone, NY) and a Nipkow-disk-based array confocal laser scanning unit, described above (CSU10, Visitron Systems) as described previously (Paltauf-Doburzynska et al., 2004; Trenker et al., 2007). All devices were controlled by Metamorph 5.0 (Visitron Systems). $[Ca^{2+}]_{\text{cyto}}$ was calculated using the following equation:

$$\left[Ca^{2+}\right]_{ER} = K_D \times \left(\frac{Ratio_{i^n} - Ratio_{min}}{Ratio_{max} - Ratio_{i^n}}\right) \mu\text{M}$$

$[Ca^{2+}]_{er}$ measurements

$D1_{ER}$ (Palmer et al., 2003) was used to monitor $[Ca^{2+}]_{ER}$ as previously described (Malli et al., 2005; Osibow et al., 2006). The FRET-based Ca^{2+} sensor $D1_{ER}$ (Palmer et al., 2003) was excited at 440±21 nm (440AF21, Omega Optical) and emission was collected simultaneously at 535 and 480 nm with one given camera using an optical beam splitter (535 and 480 nm, Dual-View MicroImager, Optical Insights, Visitron Systems). $[Ca^{2+}]_{ER}$ was calculated from the normalized ratios values:

$$Ratio_{i^n} = \left(\frac{\left(F_i^{535}/F_i^{480}\right)}{\left(F_0^{535}/F_0^{480}\right)}\right)$$

using the following equation:

$$\left[Ca^{2+}\right]_{\text{cyto}} = K_D \times \left(\frac{Ratio_i - Ratio_{min}}{Ratio_{max} - Ratio_i}\right) \mu\text{M}$$

(Osibow et al., 2006).

Statistics

Statistical data are presented as mean ± s.e.m. Analysis of variance (ANOVA) and Scheffe's post hoc *F* test were used for evaluation of the statistical significance. $P<0.05$ was defined as significant.

Supplementary Material

Refer to Web version on PubMed Central for supplementary material.

Acknowledgments

We thank Mrs Anna Schreilechner for her excellent technical assistance, Ms Karin Osibow for her critical review of this manuscript, Dr R. Tsien (University of California/San Diego, USA) for $D1_{ER}$ and Dr C. J. S. Edgell (University of North Carolina, Chapel Hill, NC, USA) for the EA.hy926 cells. This work was supported by the Austrian Science Funds (FWF, P20181-B05 and F3010-B05) and by the Franz-Lanyar-Stiftung.

References

Bauer MC, O'Connell D, Cahill DJ, Linse S. Calmodulin binding to the polybasic C-termini of STIM proteins involved in store-operated calcium entry. Biochemistry. 2008; 47:6089–6091. [PubMed: 18484746]

Berridge MJ, Lipp P, Bootman MD. The versatility and universality of calcium signalling. Nat. Rev. Mol. Cell. Biol. 2000; 1:11–21. [PubMed: 11413485]

Chevesich J, Kreuz AJ, Montell C. Requirement for the PDZ domain protein, INAD, for localization of the TRP store-operated channel to a signaling complex. Neuron. 1997; 18:95–105. [PubMed: 9010208]

Dziadek MA, Johnstone LS. Biochemical properties and cellular localisation of STIM proteins. Cell Calcium. 2007; 42:123–132. [PubMed: 17382385]

Frieden M, Malli R, Samardzija M, Demaurex N, Graier WF. Subplasmalemmal endoplasmic reticulum controls K_{Ca} channel activity upon stimulation with a moderate histamine concentration in a human umbilical vein endothelial cell line. J. Physiol. 2002; 540:73–84. [PubMed: 11927670]

Gilabert JA, Parekh AB. Respiring mitochondria determine the pattern of activation and inactivation of the store-operated Ca^{2+} current I_{CRAC}. EMBO J. 2000; 19:6401–6407. [PubMed: 11101513]

Graier WF, Groschner K, Schmidt K, Kukovetz WR. SK and F 96365 inhibits histamine-induced formation of endothelium-derived relaxing factor in human endothelial cells. Biochem. Biophys. Res. Commun. 1992; 186:1539–1545. [PubMed: 1510680]

Graier WF, Simecek S, Sturek M. Cytochrome P450 mono-oxygenase-regulated signalling of Ca^{2+} entry in human and bovine endothelial cells. J. Physiol. 1995; 482:259–274. [PubMed: 7536247]

Graier WF, Paltauf-Doburzynska J, Hill BJ, Fleischhacker E, Hoebel BG, Kostner GM, Sturek M. Submaximal stimulation of porcine endothelial cells causes focal Ca^{2+} elevation beneath the cell membrane. J. Physiol. 1998; 506:109–125. [PubMed: 9481676]

Grigoriev I, Gouveia SM, van der Vaart B, Demmers J, Smyth JT, Honnappa S, Splinter D, Steinmetz MO, Putney JW, Hoogenraad CC, et al. STIM1 is a MT-plus-end-tracking protein involved in remodeling of the ER. Curr. Biol. 2008; 18:177–182. [PubMed: 18249114]

Hewavitharana T, Deng X, Soboloff J, Gill DL. Role of STIM and Orai proteins in the store-operated calcium signaling pathway. Cell Calcium. 2007; 42:173–182. [PubMed: 17602740]

Europe PMC Funders Author Manuscripts

Hoth M, Fanger CM, Lewis RS. Mitochondrial regulation of store-operated calcium signaling in T lymphocytes. J. Cell Biol. 1997; 137:633–648. [PubMed: 9151670]

Jousset H, Malli R, Girardin N, Graier WF, Demaurex N, Frieden M. Evidence for a receptor-activated Ca^{2+} entry pathway independent from Ca^{2+} store depletion in endothelial cells. Cell Calcium. 2008; 43:83–94. [PubMed: 17548108]

Liou J, Kim ML, Heo WD, Jones JT, Myers JW, Ferrell JE Jr, Meyer T. STIM is a Ca^{2+} sensor essential for Ca^{2+}-store-depletion-triggered Ca^{2+} influx. Curr. Biol. 2005; 15:1235–1241. [PubMed: 16005298]

Liou J, Fivaz M, Inoue T, Meyer T. Live-cell imaging reveals sequential oligomerization and local plasma membrane targeting of stromal interaction molecule 1 after Ca^{2+} store depletion. Proc. Natl. Acad. Sci. USA. 2007; 104:9301–9306. [PubMed: 17517596]

Malli R, Frieden M, Osibow K, Graier WF. Mitochondria efficiently buffer subplasmalemmal Ca^{2+} elevation during agonist stimulation. J. Biol. Chem. 2003a; 278:10807–10815. [PubMed: 12529366]

Malli R, Frieden M, Osibow K, Zoratti C, Mayer M, Demaurex N, Graier WF. Sustained Ca^{2+} transfer across mitochondria is essential for mitochondrial Ca^{2+} buffering, store-operated Ca^{2+} entry, and Ca^{2+} store refilling. J. Biol. Chem. 2003b; 278:44769–44779. [PubMed: 12941956]

Malli R, Frieden M, Trenker M, Graier WF. The role of mitochondria for Ca^{2+} refilling of the ER. J. Biol. Chem. 2005; 280:12114–12122. [PubMed: 15659398]

Malli R, Frieden M, Hunkova M, Trenker M, Graier WF. Ca^{2+} refilling of the endoplasmic reticulum is largely preserved albeit reduced Ca^{2+} entry in endothelial cells. Cell Calcium. 2007; 41:63–76. [PubMed: 16824596]

Mercer JC, DeHaven WI, Smyth JT, Wedel B, Boyles RR, Bird GS, Putney JW. Large store-operated calcium selective currents due to co-expression of Orai1 or Orai2 with the intracellular calcium sensor, Stim1. J. Biol. Chem. 2006; 281:24979–24990. [PubMed: 16807233]

Muik M, Frischauf I, Derler I, Fahrner M, Bergsmann J, Eder P, Schindl R, Hesch C, Polzinger B, Fritsch R, et al. Dynamic coupling of the putative coiled-coil domain of ORAI1 with STIM1 mediates ORAI1 channel activation. J. Biol. Chem. 2008; 283:8014–8022. [PubMed: 18187424]

Nilius B, Droogmans G, Wondergem R. Transient receptor potential channels in endothelium: solving the calcium entry puzzle? Endothelium. 2003; 10:5–15. [PubMed: 12699072]

Osibow K, Malli R, Kostner GM, Graier WF. A new type of non-Ca^{2+}-buffering apo(a)-based fluorescent indicator for intraluminal Ca^{2+} in the endoplasmic reticulum. J. Biol. Chem. 2006; 281:5017–5025. [PubMed: 16368693]

Palmer AE, Jin C, Reece JC, Tsien RY. Bcl-2-mediated alterations in endoplasmic reticulum Ca^{2+} analyzed with an improved genetically encoded fluorescent sensor. Proc. Natl. Acad. Sci. USA. 2004; 101:17404–17409. [PubMed: 15585581]

Paltauf-Doburzynska J, Malli R, Graier WF. Hyperglycemic conditions affect shape and Ca^{2+} homeostasis of mitochondria in endothelial cells. J. Cardiovasc. Pharmacol. 2004; 44:424–436.

Parekh AB. Store-operated Ca^{2+} entry: dynamic interplay between endoplasmic reticulum, mitochondria and plasma membrane. J. Physiol. 2003; 547:333–348. [PubMed: 12576497]

Parekh AB, Putney JWJ. Store-operated calcium channels. Physiol. Rev. 2005; 85:757–810. [PubMed: 15788710]

Peinelt C, Vig M, Koomoa DL, Beck A, Nadler MJ, Koblan-Huberson M, Lis A, Fleig A, Penner R, Kinet JP. Amplification of CRAC current by STIM1 and CRACM1 (Orai1). Nat. Cell Biol. 2006; 8:771–773. [PubMed: 16733527]

Putney JW Jr. A model for receptor-regulated calcium entry. Cell Calcium. 1986; 7:1–12. [PubMed: 2420465]

Putney JW Jr. Capacitative calcium entry revisited. Cell Calcium. 1990; 11:611–624. [PubMed: 1965707]

Roos J, DiGregorio PJ, Yeromin AV, Ohlsen K, Lioudyno M, Zhang S, Safrina O, Kozak JA, Wagner SL, Cahalan MD, et al. STIM1, an essential and conserved component of store-operated Ca^{2+} channel function. J. Cell Biol. 2005; 169:435–445. [PubMed: 15866891]

Smyth JT, DeHaven WI, Bird GS, Putney JW. Role of the microtubule cytoskeleton in the function of the store-operated Ca^{2+} channel activator STIM1. J. Cell Sci. 2007; 120:3762–3771. [PubMed: 17925382]

Trenker M, Malli R, Fertschai I, Levak-Frank S, Graier WF. Uncoupling-proteins 2 and 3 are elementary for mitochondrial Ca^{2+} uniport. Nat. Cell Biol. 2007; 9:445–452. [PubMed: 17351641]

Yi M, Weaver D, Hajnoczky G. Control of mitochondrial motility and distribution by the calcium signal: a homeostatic circuit. J. Cell Biol. 2004; 167:661–672. [PubMed: 15545319]

Yuan JP, Zeng W, Huang GN, Worley PF, Muallem S. STIM1 heteromultimerizes TRPC channels to determine their function as store-operated channels. Nat. Cell Biol. 2007; 9:636–645. [PubMed: 17486119]

Zhang SL, Yeromin AV, Zhang XH, Yu Y, Safrina O, Penna A, Roos J, Stauderman KA, Cahalan MD. Genome-wide RNAi screen of Ca^{2+} influx identifies genes that regulate Ca^{2+} release-activated Ca^{2+} channel activity. Proc. Natl. Acad. Sci. USA. 2006; 103:9357–9362. [PubMed: 16751269]

Europe PMC Funders Author Manuscripts

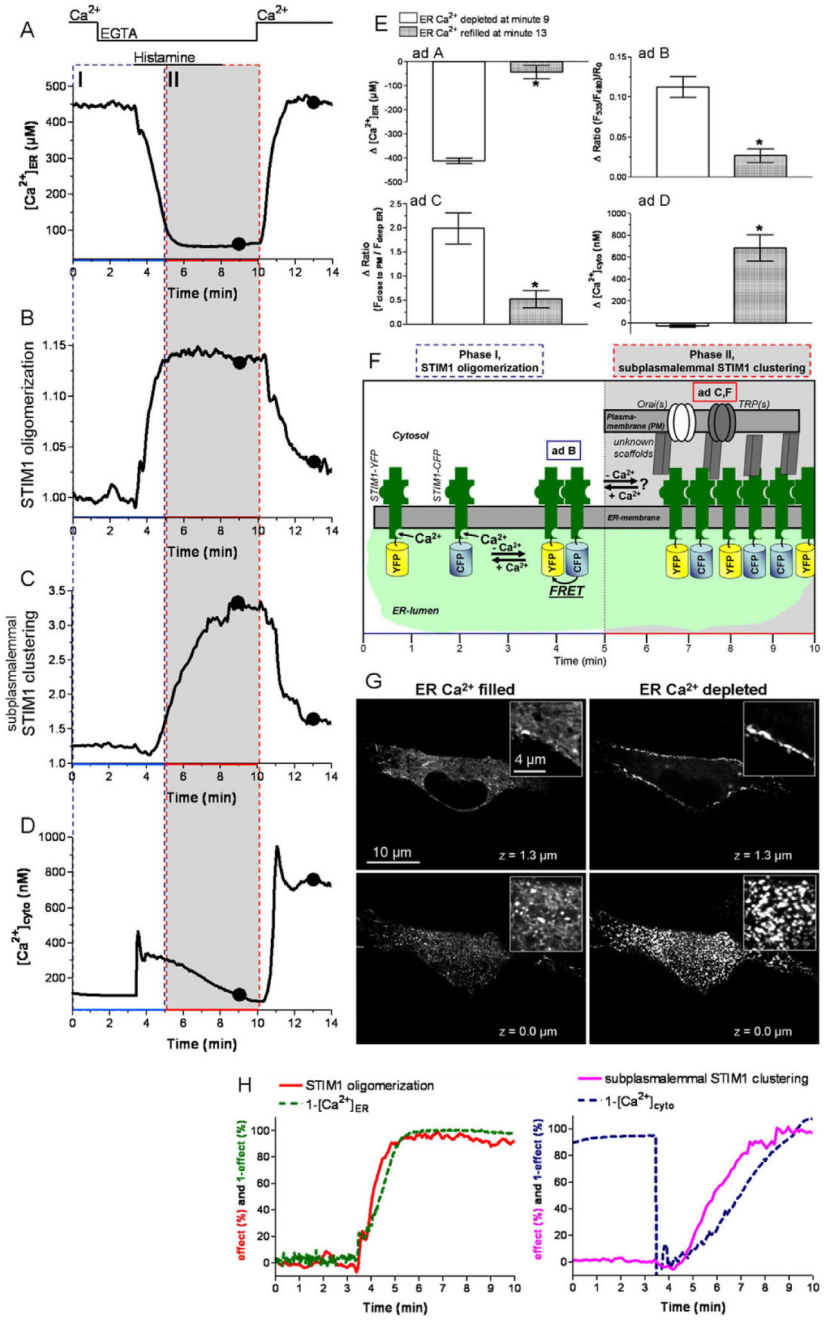

Fig. 1. STIM1 oligomerization upon maximal ER Ca^{2+} depletion correlated with ER Ca^{2+} depletion, while subplasmalemmal STIM1 clustering was delayed and followed the decay of cytosolic Ca^{2+} levels.

(A-D) Representative tracings of the effect of 100 μM histamine on $[Ca^{2+}]_{ER}$ (A), STIM1 oligomerization (B), subplasmalemmal STIM1 clustering (C) and $[Ca^{2+}]_{cyto}$ (D) in EGTA-containing solution followed by re-addition of 2 mM Ca^{2+} in the absence of histamine. (E) Respective statistical evaluation of the experiments displayed in A (*n*=11), B (*n*=7), C (*n*=12) and D (*n*=12). (F) Schematic illustration of STIM1 activation by ER Ca^{2+} depletion. (G) Images of the subcellular distribution of YFPSTIM1 under conditions of high ER Ca^{2+}

Europe PMC Funders Author Manuscripts

levels in resting cells (left images) and low ER Ca^{2+} levels upon cell stimulation with histamine in EGTA (right images) at the middle *z*-plane (upper images) and at a TIRF-like bottom plane (lower images). (H) Normalized tracings of $[Ca^{2+}]_{ER}$ and $[Ca^{2+}]_{cyto}$ were inverted and plotted with the respective normalized traces for STIM1 oligomerization and STIM1 clustering (Δ_{max}=100%).*P<0.05 versus the respective compared data set.

Europe PMC Funders Author Manuscripts

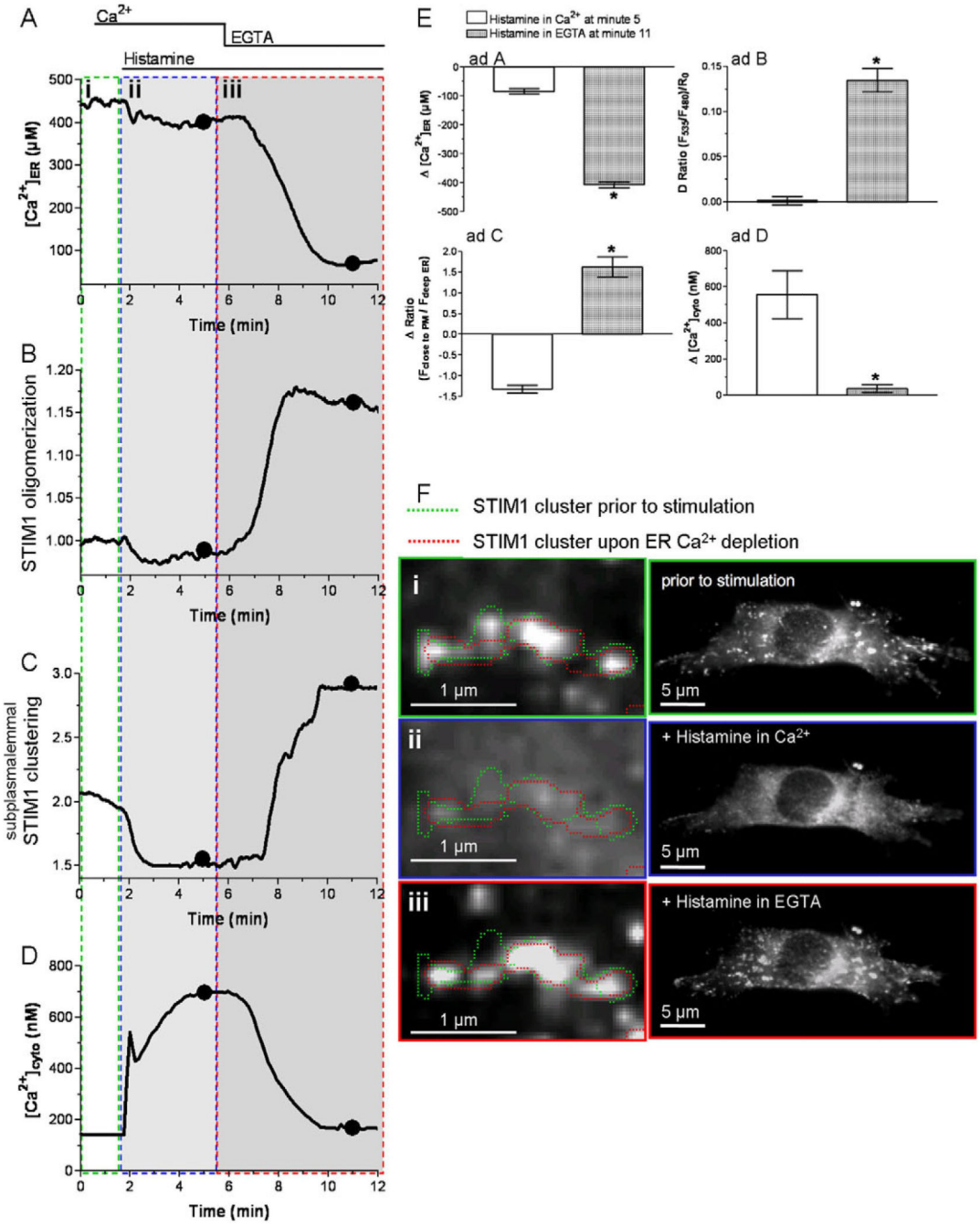

Fig. 2. The dynamics of STIM1 oligomerization and subplasmalemmal clustering upon moderate and strong ER Ca^{2+} depletion was limited, while subplasmalemmal STIM1 clustered repetitively at focal points.

(A-D) Representative tracings of the effect of 100 μM histamine on $[Ca^{2+}]_{ER}$ (A), STIM1 oligomerization (B), subplasmalemmal STIM1 clustering (C) and $[Ca^{2+}]_{cyto}$ (D) in Ca^{2+}-containing buffer followed by removal of Ca^{2+} in the presence of histamine. (E) Respective statistical evaluation of the experiments displayed in A (*n*=12), B (*n*=8), C (*n*=6) and D (*n*=6). (F) Spatial reversibility of subplasmalemmal STIM1 clusters and the histamine-induced degradation of pre-existing STIM1 clusters: i, pre-existing STIM1 clusters under

resting conditions; ii, histamine induced disassembly of STIM1 cluster; iii, reassembly of STIM1 clusters upon removal of extracellular Ca^{2+}.

Europe PMC Funders Author Manuscripts

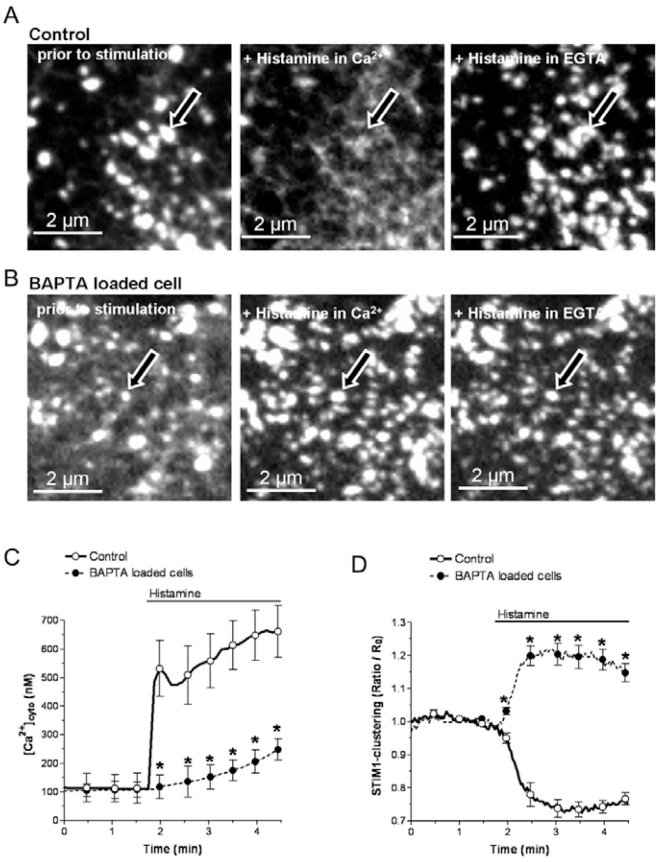

Fig. 3. BAPTA-am loading reversed the disassembly of STIM1 clusters by histamine.

(A) Representative images of the sensitivity of pre-existing subplasmalemmal STIM1 clusters to histamine and their recovery upon reduction of $[Ca^{2+}]_{cyto}$ (n=6). (B) BAPTA reversed the decomposition of preexisting subplasmalemmal STIM1 clusters upon histamine stimulation independently from extracellular Ca^{2+} (n=6). (C,D) Cytosolic Ca^{2+} signaling (C) and kinetics of subplasmalemmal STIM1 clustering (D) in response to 100 µM histamine in the presence of 2 mM extracellular Ca^{2+} in YFP-STIM1-expressing cells that were loaded with either fura-2-am (n=6) or with fura-2-am and BAPTA-am (n=6). *P<0.05 versus the respective compared data set.

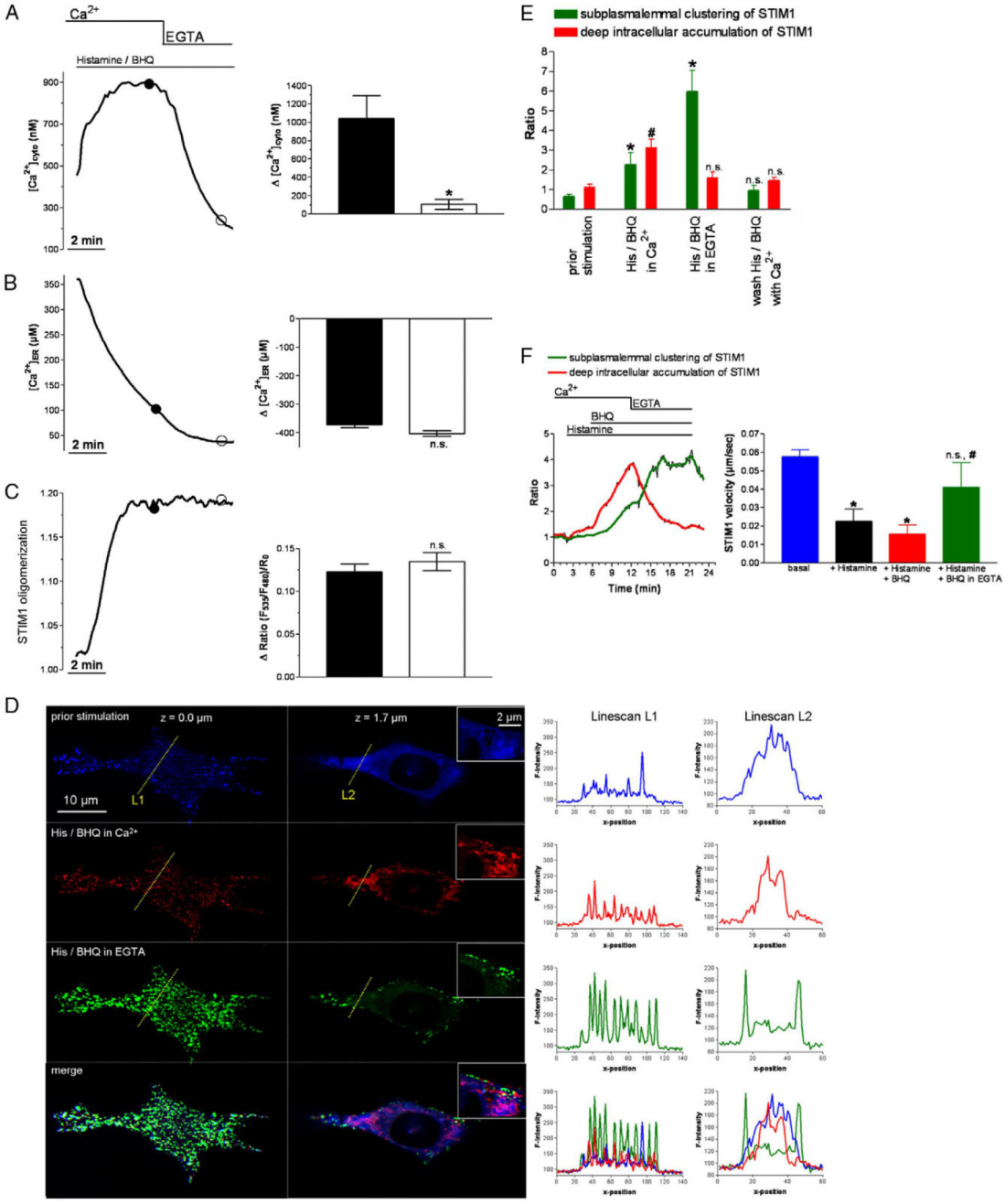

Fig. 4. STIM1 oligomerization and STIM1 clustering upon strong ER Ca^{2+} depletion, impeded ER Ca^{2+} replenishment at high and low $[Ca^{2+}]_{cyto}$ levels.

(A-C) Representative tracings (left graphs) and statistical summary (right graphs) of $[Ca^{2+}]_{cyto}$ (A, *n*=12), $[Ca^{2+}]_{ER}$ (B, *n*=9) and STIM1 oligomerization (C, *n*=28) in response to stimulation with 100 µM histamine and the SERCA inhibitor BHQ (15 µM). (D) Subcellular distribution of STIM1 at a TIRF-like plane (left images) and at a middle *z*-plane (right images) under resting conditions ('prior stimulation', upper panel), under cell stimulation with 100 µM histamine and 15 µM BHQ in 2 mM Ca^{2+} ('His/BHQ in Ca^{2+}', upper middle panel) and cell stimulation in EGTA ('His/BHQ in EGTA', lower middle

panel). Along the lines indicated, fluorescence intensity of YFP-STIM1 is presented at the corresponding *z*-plane and activation stages in the right graphs. The lower images and graphs show overlays of the upper illustrations. (E) Average data and respective statistical evaluation of the experiments displayed in D (n=11 for each condition). (F) The time course of STIM1 clustering (n=3 for each condition). *P<0.05 versus the respective compared data set.

Europe PMC Funders Author Manuscripts